Submitted to: **Engineering Geology (ENGEO4476-revised draft)**

# Undrained shear behavior of loess saturated with different concentrations of sodium chloride solution

Fanyu Zhang[a,b], Gonghui Wang[a,*], Toshitaka Kamai[a], Wenwu Chen[b],

Dexuan Zhang[c], Jun Yang[d]

Affiliations:

(a):

Research Center on Landslides
Disaster Prevention Research Institute
Kyoto University
Gokasho, Uji, Kyoto, 611-0011
Japan

(b):
Key Laboratory of Mechanics on Disaster and Environment in Western China (Lanzhou University), Ministry of Education, China
Department of Geological Engineering
Lanzhou University
Tianshui Road, 222, Lanzhou, 730000
P.R. China

(c):
Department of Civil Engineering
Shanghai Jiao Tong University
Shanghai 200240
P.R. China

(d):
Department of Civil Engineering
The University of Hong Kong
Hong Kong
P.R. China

*: Corresponding author
Email: wanggh@landslide.dpri.kyoto-u.ac.jp
Telephone: +81-774-384115; Fax: +81-774-384300

# Undrained shear behavior of loess saturated with different concentrations of sodium chloride solution

Fanyu Zhang[a,b], Gonghui Wang[a,*], Toshitaka Kamai[a], Wenwu Chen[b], Dexuan Zhang[c], Jun Yang[d]

**Abstract**: A series of ring-shear tests was conducted on saturated loess to investigate the effects of NaCl concentration in pore water and desalinization on the shear behavior under undrained conditions. The loess samples were taken from the ground surface of a frequently active landslide in China, were saturated by de-aired, distilled water with different concentrations of NaCl, and then were sheared undrained. After that, the samples were retrieved, remoulded, re-set into the shear box, and re-saturated by passing through de-aired, distilled water such that the samples were desalinized, and then were sheared undrained again. Through comparing the undrained shear behavior, the effects of NaCl in the pore-water and desalinization on the undrained shear behavior of loess were examined. The results showed that the variation of NaCl concentration in pore water can strongly affect the shear behavior of saturated loess. Both the peak shear strength and steady-state strength increased with increase of NaCl concentration until a certain value, after which they decreased with further increase of NaCl concentration. Meanwhile, the peak shear strength and steady-state strength of the desalinized samples recovered to those of the original sample; hence, the effects of salinization are reversible. These findings may be of practical importance to better understanding the repeated occurrence of some irrigation-induced loess landslides in China.

Keywords: sodium chloride; loess landslide; undrained shear behavior; irrigation

## 1. Introduction

Landslides are very serious geohazards in the Chinese Loess Plateau because they cause serious casualties and destruction almost every year. These loess landslides exhibit a great diversity of movement modes and rates (Derbyshire, 2001), ranging from imperceptibly continuous creep to instantaneously rapid flow. It has been recognized that the movement of most of these landslides is triggered by a reduction in shear strength in loess (Derbyshire et al., 1994; Dijkstra et al., 1994; Zhang and Wang, 2007; Zhang et al., 2009). Although water content has been identified as a key factor in influencing the shear strength behavior of loess (Gibbs and Holland, 1960; Derbyshire et al., 1994; Zhang et al., 2009; Picarelli, 2010), it has also been suggested that the salinity in pore water can strongly modify the shear strength of loess (Dijkstra et al., 1994). Furthermore, high salt concentrations in groundwater and significant soil salinization have been observed in the Chinese loess area, especially those areas involving agricultural irrigation (Chen et al., 1999; Long et al., 2007; Xu et al., 2011a).

The effect of salt concentration in pore water on shear strength has been investigated for better understanding the mechanism of slope failure in mudstone or clays (Steward and Cripps, 1983; Moore, 1991; Di Maio and Fenelli, 1994; Anson and Hawkins, 1998; Tiwari et al., 2005; Gajo and Maines, 2007; Wahid et al., 2011). These studies have found that changing pore water salinity can modify the shear strength of the soils. Although the effect of salt concentration on the shear strength of clays has thus been widely examined, studies on natural soils are rare and need further scrutiny (Di Maio, 1996), and little effort has been

made to understand salinity effects on shear strength of silty soil, such as loess. Furthermore, the effects of salt concentration on the initiation and movement of loess landslides remains unclear.

In this research a series of ring-shear tests was conducted on loess samples that were taken from the ground surface of an irrigation-induced landslide on Heifangtai terrace located 40 km west of Lanzhou City, Gansu Province, China (Fig. 1). The objective of this research is to investigate the possible effects of different concentrations of NaCl solution and desalinization on the shear behavior of saturated loess under undrained conditions, because we found that pore water chemistry fluctuates in the region from seasonal agricultural irrigation activities. We prepared the loess samples by saturating them using de-aired, distilled NaCl solutions with different concentrations, and then sheared them in undrained condition. After the tests, we retrieved and dried the samples and remoulded them into the shear box, re-saturated them by passing through de-aired, distilled water to remove NaCl from the samples, and then sheared them undrained. By comparing the undrained shear behaviors, the effects of NaCl solution as the pore fluid and desalinization were examined. Liquid limit, and scanning electron microscopy (SEM) images of loess samples saturated by NaCl solution were studied to examine the possible change in soil structure due to the addition of NaCl. Based on our findings, we analyzed the possible mechanisms for the repeated occurrence of landslides on the loess terrace of Heifangtai, China during irrigation periods.

## 2 Study site

Heifangtai terrace (Fig. 1) has an area of 13.7 $km^2$ and was built as a farm land for residents relocated there from the reservoir area created by the construction of Liujiaxia dam on the Yellow River. Farms on the terrace require irrigation from Yellow River, which began in 1969. The irrigated area is about 7.53 $km^2$ (Wang et al., 2004; Xu et al., 2011b). Normally, irrigation occurs during five events every year following the requirements for the crops, and the annual amount of irrigation water ranges between $6.0\times10^6$ $m^3$ - $8.0\times10^6$ $m^3$, corresponding to a total depth of water of 438 - 584 mm. From 1971 to 2000, the annual precipitation averaged about 300 mm, 71% of which fell between June and September, while annual evaporation averaged approximately 1700 mm (Wang et al., 2004). Clearly, the irrigation water plays a critical role in recharge and variation of groundwater in the terrace.

The lithological profile of Heifangtai can be divided into four units (Fig. 2) (Wang et al., 2004; Xu et al., 2011b). The upper layer (about 25-50 m thick) is made up of Malan loess and Lishi loess. Malan and Lishi loess were accumulated during Holocene and Middle-Late Pleistocene, respectively. A clay layer (4~17 m thick) underlies the loess layer. Below the clay layer are alluvial deposits (2~5 m thick), consisting mainly of well-rounded pebbles sized approximately 5-10 cm in diameter. The bedrock is mainly composed of mudstone and sandy mudstone with minor sandstone and conglomerate.

The clay underlying the loess forms a nearly impermeable layer at Heifangtai, and springs flow out from the plateau face at the interface between the loess and clay layers. Largely due to long-term irrigation, a water bearing strata (about 20 m thick) has formed on the bottom of

the loess layer and colluvial deposits, and the volume of springs from the Heifangtai area rose from $3.2 \times 10^4$ $m^3$ before the irrigation to $91.5 \times 10^4$ $m^3$ in 2000 (Wang et al., 2004). Associated with the rising perched water table, loess landslides frequently occurred within the terrace since 1984, causing great loss of lives and properties. During the period of 1984 to 2000, at least sixty large landslide events occurred, and more than half of them in March and July (Wang et al., 2004). The terrace has become a representative case of irrigation-induced loess landslides in the Chinese Loess Plateau.

Chemical composition analyses have shown that the concentrations of various ions in the irrigation water from Yellow River are lower than those in the groundwater, spring water, and soil of the Heifangtai terrace (Table 1) (Chen et al., 1999). Among those ions measured in terrace soils and water, sodion ($Na^+$) and chloridion ($Cl^-$) are predominant (>70% of the total ions). Concentrations are sufficiently high to form salt deposits that can be observed on the surface of soil layers on the toe part of the side slope of the terrace when the soil layers become dry (white colored parts in Fig. 3), while these deposits normally disappear during the irrigation season (Fig. 1c).

## 3 Materials and methods

### 3.1 Test samples

To examine the possible effects of pore water NaCl on the shear behavior of loess, we took loess samples from the ground surface of a landslide in the Heifangtai terrace (Fig. 1b). The loess consists mainly of silt (about 94%, Fig. 4) with some clay (about 6%). The mean

particle diameter is 0.02 mm and the coefficient of uniformity is 5.0. The minerals are predominantly quartz and feldspar with a small amount of mica, kaolinite and illite (Zhang, 2007). Some basic physical properties of the sample taken from the field are listed in Table 2.

### 3.2 Solutions

Because $Na^+$ and $Cl^-$ are the predominant ions in the groundwater, spring water, and soil mass (Table 1), we used solutions of sodium chloride (NaCl) to saturate the loess samples in this research. To examine the effect of salt concentration in pore water, NaCl was dissolved in de-aired distilled water to the desired concentrations (i.e., 3, 6, 10, 12, 14 and 16% by weight). Hereinafter, we term these NaCl solutions with the concentrations being 3%, 6%, 10%, 12%, 14% and 16% as $S_3$, $S_6$, $S_{10}$, $S_{12}$, $S_{14}$ and $S_{16}$, respectively, and term the de-aired distilled water as $S_0$.

### 3.3 Ring shear apparatus

The ring shear apparatus has been widely used in examining the residual shear strength of soils for the analysis of slope stability (e.g., Bishop et al., 1971; Bromhead, 1979; Sassa et al., 2004; Wang and Sassa, 2009; Wang et al., 2010). The ring shear apparatus employed in the present research is the fifth version (DPRI-5) developed by the Disaster Prevention Research Institute (DPRI), Kyoto University (Sassa et al., 2004), and has a shear box (Fig. 5) sized 120 mm in inner diameter, 180 mm in outer diameter and 115 mm in height. This apparatus enables the simulation of many different kinds of static and dynamic loading under drained or undrainded conditions. The samples can be using controlled torque or controlled shear speed.

Fig. 5 presents a schematic of this apparatus. The overview of the apparatus is shown in Fig. 5a. The shear mode of a sample in the ring-shear apparatus is shown conceptually in Fig. 5b. The sample in the ring-shear box is doughnut shaped and is laterally confined between pairs of upper and lower confining rings. During the test, the sample is loaded normally through an annular loading platen connected to a load piston. The lower half of the shear box rotates in both directions, driven by a servomotor through a transmission system, while the upper part is kept steady by means of two retaining torque arms. The shear resistance is measured by means of these two torque arms. Fig. 5c illustrates an enlarged diagram of half of the cross section of the ring-shear box and the pore-water pressure measurement system. Further detailed information on ring shear tests can be found from relevant literature (e.g., Wang and Sassa, 2002; Sassa et al., 2003).

### 3.4 Testing program and procedure

Firstly, we performed a series of tests to examine the possible effect of NaCl concentration in pore water on the shear behavior of loess. In this series, seven samples ($T_1$ to $T_7$ in Table 3) were prepared with the same initial void ratio and consolidating stress, but saturated by NaCl solution of different concentrations. It is noted that test $T_7$' in Table 3 was performed to ensure the repeatability of the test by using higher NaCl concentration, although at which the initial density of the sample differed from that in $T_7$.

Secondly, a series of experiments was performed to examine the possible effect of desalinization of the loess samples that had been saturated previously by NaCl solutions, and

also to check the reversibility of NaCl effects. The samples were retrieved carefully from the shear box after tests $T_1$ - $T_7$ were finished, were oven-dried, disaggregated using a rubber hammer, replaced into the shear box, and finally re-saturated by passing through de-aired, distilled water to remove the NaCl solution introduced during tests $T_1$ - $T_7$. Six tests ($T_8$ - $T_{13}$, Table 3) were conducted in this series with the initial void ratios and consolidating stresses being approximately the same as those in tests $T_1$ - $T_7$. During preparation for tests $T_8$ - $T_{13}$, ~50 g of loess was added to each sample because of sample loss during retrieval from the specimen chamber following tests $T_2$ – $T_7$.

During the preparation of samples for each test series, distilled water was first added to the oven dried, disaggregated loess to reach an initial water content of 5%, and then the samples were stirred evenly by hand. Thereafter, the samples were sealed using thin plastic film and stored for 24 hours in an air-conditioned room to achieve uniform distribution of moisture. After that, the samples were placed into the shear box and prepared following the moist tamping method (Ishihara, 1993). To achieve uniform density, the samples were placed in three layers, and each layer was tamped such that a designed void ratio was achieved. The samples were saturated with the help of carbon dioxide and de-aired NaCl solutions for the first test series, and carbon dioxide and de-aired, distilled water for the second series. In all the tests, the degree of saturation was checked by measuring the $B_D$ parameter, which was proposed by Sassa (1985) for use in the direct-shear state. The $B_D$ is defined as the ratio between the increment of generated excess pore pressure ($\Delta u$) and normal stress ($\Delta \sigma$) in the undrained condition, and formulated as $B_D = \Delta u/\Delta \sigma$. If $B_D \geq 0.95$, this indicates that the

sample is approximately fully saturated. In this study, all samples were saturated with $B_D \geq 0.95$. After checking the $B_D$ parameter, the sample was consolidated under a normal stress of 250 kPa without applying any shear stress, and then was sheared by increasing the shear stress at a loading rate of 0.098 kPa/s (0.001 $kgf \cdot cm^{-2} \cdot s^{-1}$) under undrained condition. All of the samples were sheared to a large shear distance (about 1 m), beyond which excess pore-water pressure and shear resistance were constant; hence, the samples were sheared to the steady state as defined by Poulos (1981).

## 4 Results

All the test results are summarized in Table 3. In all of the undrained shear tests, the samples exhibited fully contractive behavior throughout the entire shearing process, i.e., the pore pressure continuously increased with the progress of shearing.

### 4.1 Typical undrained shear behavior

To exemplify the shear behavior observed in all tests, the results of three tests ($T_1$, $T_5$ and $T_{11}$ in Table 3) are presented in Figs. 6 - 8. These tests were performed using $S_0$ ($T_1$, Fig. 6), $S_{12}$ ($T_5$, Fig. 7), and $S_0$ after desalinizing the $T_5$ sample ($T_{11}$, Fig. 8). Figs. 6a, 7a and 8a present the normal stress, shear resistance, and pore pressure against shear displacement, and Figs. 6b, 7b and 8b plot the time series data of normal stress, shear resistance, and pore pressure. In Figs 6a, 7a and 8a, to facilitate a clearer view of the generation of pore pressure accompanying the shear displacement in the initial shearing period, a logarithmic abscissa of

shear displacement was used for displacement ≤ 0.1 m was taken, and a linear abscissa was used above this value to show that the test had been sheared to steady state (point SSP). It can be seen that some pore-water pressure was built-up before the peak shear strength was mobilized (point F), while after the onset of failure, pore-water pressure showed a sharp increase and shear strength underwent a quick reduction. This period is usually known as the collapse period, mainly due to the failure of the meta-stable structure (Wang and Sassa, 2002). Afterwards, with further increase in shear displacement, pore-water pressure and shear resistance gradually trended to constant levels. Figs. 6c, 7c and 8c illustrate the effective stress path. It can be seen that in each test, the effective stress path tended leftward with increasing shear stress, and finally reached their respective peak shear strength (point F), thereafter the path descended towards its steady-state strength (point SSP). The results shown in Figs. 6-8 reveal that NaCl in pore water can influence the undrained shear behavior of saturated loess, and the influence of salinization can also be eliminated by desalinization.

### 4.2 Effects of NaCl concentration

Seven samples ($T_1$-$T_7$, Table 3) were prepared at the same initial void ratio but saturated by different de-aired solutions of $S_0$, $S_3$, $S_6$, $S_{10}$, $S_{12}$, $S_{14}$, and $S_{16}$, respectively, to examine the effect of NaCl concentration in pore water on the undrained shear behavior. Test results are provided in Fig. 9.

Figs. 9a-b present the corresponding variation of shear resistance and pore-water pressure with shear displacement, and Fig. 9c plots the effective stress paths. From Figs. 9a-b, we

found that at a given shear displacement, the corresponding shear resistance became greater and the excess pore water pressure became smaller with increasing NaCl concentration in the solution from 0% to 12%. However, with further increase of NaCl concentration, shear resistance became smaller and excess pore-water pressure became greater. The peak and residual shear strengths showed the same relations to variations of NaCl concentration. At NaCl concentrations of 0-12%, the peak shear strength and steady-state shear strength increased with increasing NaCl concentration (Fig. 9c), whereas peak and steady-state shear strength decreased with increasing NaCl concentration greater than 12%. In addition, the effective stress paths showed an arc and convex shape for all of the seven tests (i.e., $T_1$ to $T_7$), although test $T_5$ results displayed a more abrupt peak than the others. The results indicate that undrained shear behavior of saturated loess is sensitive to the NaCl concentrations of pore-water.

### 4.3 Effects of desalinization

Shear tests on clay have demonstrated that the shear strength decreases with decreasing pore water salt concentration due to desalinization (Di Maio and Fenelli, 1994; Di Maio, 1996; Tiwari et al., 2005, Wen and He, 2012). However, the effect of desalinization on the shear behavior of loess is unclear. To study the effects of desalinization on the undrained shear behavior of loess and to examine the reversibility of NaCl effects, a series of tests was conducted involving desalinization of samples retrieved following tests $T_2$-$T_7$. The desalinization process was conducted by saturating the salty samples with de-aired distilled

232 water. Six tests were performed and their results are summarized in Table 3, and presented in
233 Fig. 10, where the results from test T1 are also included.
234 Figs. 10a and 10c show that the undrained shear behaviors for the tests were very similar,
235 although small differences exist. These differences may result from small variations of initial
236 densities between the tests, and also from possible incompletion of the desalinization process.
237 Figs. 9 and 10 indicate that desalinization reduces shear strength, while the process of
238 salinization followed by desalinization has very little, if any, influence on the undrained shear
239 behavior. Hence, desalinization can lower the shear strength of loess saturated by NaCl
240 solutions, and the effects of salinization are reversible. These findings are consistent with
241 those for clays with NaCl solutions as pore water (Di Maio and Fenelli, 1994; Di Maio, 1996;
242 Tiwari et al., 2005).
243
244 **5. Discussion**
245 **5.1 Undrained peak shear strength and steady-state strength**
246 The undrained peak shear strength is usually considered to reflect the potential
247 resistance to liquefaction for a saturated sample, whereas the steady-state strength plays an
248 important role in the post-failure behavior of a liquefied soil mass (Wang et al., 2007). It
249 has been found that the peak shear strength is dependent on the initial stress state and the
250 density of a soil (Kramer, 1988; Wang et al., 2007), as well as the fine particle content of a
251 soil (Wang et al., 2007); whereas the steady-state strength is related only to the type of the
252 soil and its density, and is independent of the initial stress state (Poulos et al., 1985; Wang

253 and Sassa, 2002; Wang et al., 2007). Because all of the tests in this research were performed
254 using the same soil under the same initial stress state and nearly identical density, variations
255 of peak shear strengths and steady-state strengths are considered to result from variations in
256 NaCl concentrations in the pore water (Table 3).

257 The peak shear strength and the steady-state strength for tests $T_1$ to $T_7$' listed in Table 3
258 are plotted against NaCl concentration in Fig. 11. It can be seen that the peak shear strength
259 and the steady-state strength initially increased with increasing NaCl concentration until a
260 maximum resistance was reached at the NaCl concentration of 12%, and then decreased
261 with further increase of NaCl concentration. It is noted that the difference in the shear
262 strength for tests $T_7$ and $T_7$'may result from the difference in their initial density. Normally,
263 denser sample will have greater peak and residual undrained shear strengths when subjected
264 to undrained shearing (Ishihara, 1993).Therefore, we concluded that test $T_7$' indirectly
265 confirmed the repeatability of test 7.

266 The peak shear strength and the steady-state strength for tests $T_1$ and $T_8$ to $T_{13}$ are
267 plotted in Fig. 12 against the NaCl concentration that existed prior to desalinization and
268 performance of the tests. It can be seen that the peak shear strengths and steady-state shear
269 strengths show very little variation, unlike the significant variations in strengths observed
270 during tests of salinized samples (Fig. 11). Therefore, from Fig. 12, we can conclude that
271 the effects of salinization are reversible through desalinization.

272

273 **5.2 Physicochemical effects**

It has been found that when the clay content in a soil is more than 10%, changes in pore water chemistry can greatly influence the shear strength of the soil (Mori, 1964; Moore, 1991; Mitchell and Soga, 2005). Studies of the shear behavior of clays have found that the variation of shear strength with salt concentration is related to the physicochemical interactions between clay particles (Kenney, 1967; Ramiah et al., 1970; Moore, 1991; Di Maio and Fenelli, 1994; Anson and Hawkins, 1998; Tiwari et al., 2005; Gajo and Maines, 2007). The physicochemical interactions can be greatly influenced by the specific surface area, which is related to the grain size distribution of the soil (Lambe and Whitman, 1969; Moore, 1991; Santamarina *et al.*, 2002; Mitchell and Soga, 2005). Generally, the smaller the particle, the greater its specific surface area. It is also known that the shear strength of a soil depends on the shear resistance at contacts between particles and the interlocking of particles. The interlocking of particles is mainly related to the packing density, and the physicochemical interactions between clay particles affect the number and the resistance of particle contacts, and thus affect the total shear strength (Lambe and Whitman, 1969; Dieterich and Kilgore, 1994).

Our test results showed that the undrained shear strength of loess with only 6% clay is also very sensitive to the pore water chemistry. Because we prepared all the samples with nearly identical initial densities and also sheared them under the same stress state, NaCl concentration in pore water was the only variable that could have caused strength variations.

The increasing tendency of both peak and residual shear strengths with increase of NaCl concentration (before a NaCl of ~ 12%) can be explained as follows. The loess is basically

295 an assembly of silt grains with clay particles being the dominant bonds. When this loess is
296 saturated by NaCl solution, due to the inward diffusion of the salt into the clay, thickness of
297 the double layer of clay particles decreases with increase in NaCl concentration in pore fluid.
298 This process will result in ion diffusion into the fluid, causing decrease of the osmotic
299 repulsion and increase of Van der Waals's attractive forces among clays (Barbour and
300 Fredlund, 1989; Mitchell, 1993; Tiwari, et al., 2005; Wen and He, 2012). However, when
301 these processes increase interparticle forces among clays, they also lead to aggregation of
302 particles coarser than clay (Tiwari, et al., 2005; Wen and He, 2012). Bigger aggregates or
303 cluster of aggregates are formed when NaCl concentration becomes greater. When the
304 bonding between coarse grains is dominated by these aggregates, larger inter-aggregate pore
305 can be formed, basically changing the fabric of sample, and then changing the undrained
306 shear behavior. Recently studies have revealed that besides of initial void ratio, fabric of the
307 sample also plays key role in the shear behavior of sands (Oda, 1972a,b; Ladd, 1974;
308 Tatsuoka et al., 1979; Zlatovic and Ishihara, 1997; Yamamuro and Lade, 1999).

309 To observe the variation of aggregate cluster formation with NaCl concentration, we
310 collected samples from the layer above the shear zone of each test specimen, and observed
311 their microstructures by using SEM techniques. Fig. 13 presents some of the SEM images,
312 which show that salt bonding between clay particles replaces the existing bonding of water
313 as NaCl concentration increases. This will result in aggregation of particles to sizes coarser
314 than clay, which elevates the shear resistance. A similar principle had been proposed to
315 explain observed variation of residual shear strength of clayey soils with different pore

316 fluids (Sridharan and Jayadeva, 1982; Sridharan and Prakash, 1999; Wen and He, 2012).
317 During our study, above a NaCl of ~ 12%, additional NaCl resulted in the formation of
318 aggregate clusters, which led to the formation of larger void spaces (see Figs. 13 e and f),
319 change the fabric of the sample. In this case, the shear behavior of the sample will be
320 dominated by the shear failure of aggregate clusters and previous studies found that soil
321 with relatively larger aggregates was weaker than soil with small aggregates (McDowell
322 and Bolton, 1998; Iverson et al., 2010).

323 Desalinized specimens had nearly identical shear strength (Fig. 12) as the original sample.
324 The reversibility of the salinization effects is due to dilution or removal of NaCl by distilled
325 water. The reversible behavior suggests that the addition of NaCl does not produce any
326 cation-exchange phenomenon, because cation exchange would cause at least partial
327 irreversibility (Di Maio, 1996, 1998).

328 Liquid limits of loess saturated by different NaCl solutions are plotted in Fig. 14. Liquid
329 limit is often used to understand effects of the variation of pore water chemistry on soil
330 shear strength, permeability and structure (Bowders and Daniel, 1987; Moore, 1991; Anson
331 and Hawkins, 1998; Gratchev and Sassa, 2009). Many previous studies on clays showed
332 that an increase in salt concentration will cause a decrease in liquid limit, and concurrently
333 an increase in shear strength (Kenney, 1967; Moore, 1991, 1992; Di Maio and Fenelli,
334 1994; Di Maio, 1996; Anson and Hawkins, 1998; Tiwari et al., 2005; Gajo and Maines,
335 2007; Wahid et al., 2011). This kind of variation of liquid limit with pore water chemistry
336 may result from the change in clay microstructure or physicochemical forces between clay

particles due to the physicochemical effects (Moore, 1991; Di Maio and Fenelli, 1994). However, Fig.15 indicates that NaCl concentration had negligible effect on liquid limit, if any. This may be due to the fact that the loess has a low clay fraction (about 6%), so the effects of the pore water chemistry on the clay has little effect on properties of the loess as a whole. From this point of view, we may conclude that liquid limit can not be always used as a qualitative indicator to evaluate the change in shear strength with pore water chemistry, because it depends mainly on the clay content and mineralogy of the soils.

### 5.3 Implications for irrigation-induced loess landslides

As shown in Figs. 9-11, the change in the concentration of salt in pore water can modify the shear behavior of loess, and thus influence the initiation and movement of loess landslides due to desalinization from irrigation. In the case of Heifangtai terrace, the long-term irrigation can elevate the groundwater table and decrease the NaCl concentration of the groundwater. Elevation of the groundwater table can reduce the effective normal stress and, consequently, lower the shear strength. Decreasing the NaCl concentration can lower both the peak and steady-state shear strength of loess as shown herein. In this sense, irrigation played a dual role in triggering landslides in the Heifangtai area. Landslides began occurring in the Heifangtai area about 20 years after the start of irrigation. This delay may be due to relatively low permeability of the thick loess layer and high evaporation that may have retarded the rise of the groundwater table. Also, desalinization from irrigation was likely time consuming and partly resulted in the delayed occurrence of the loess landslides.

358 The seasonality of landslides in the Heifangtai area supports the conclusion that they are
359 caused by desalinization and consequent strength loss; landslides mostly occur during
360 March and July when irrigation and rainfall amounts are greatest.
361
362 **6. Conclusions**
363 A series of ring-shear tests was conducted on Chinese loess to assess the effects of
364 NaCl concentration in pore water on its undrained shear behavior. Based on the test results,
365 the following conclusions can be drawn:
366 (1) The undrained shear behavior of saturated loess is sensitive to the concentration of
367 NaCl in pore water, and the variation of NaCl concentrations has a significant influence on
368 both the peak shear strength and steady-state strength.
369 (2) The peak shear strength and steady-state strength increase as pore water NaCl
370 concentration increases to 12% by weight. Above this concentration, both strengths
371 decrease with further increase in the NaCl concentration.
372 (3) The properties of salinized loess are reversible by desalinization. After being
373 desalinized, the loess samples showed almost identical shear behavior to that of the original,
374 non-salinized loess sample.
375 (4) The periodic irrigation of the Heifangtai area may change the NaCl concentration in
376 the groundwater and, hence, the shear strength of the loess. With irrigation and abundant
377 rainfall, desalinization occurs along with consequent lowering of peak shear strength, which

may facilitate the triggering of landslides. Lowered steady-state shear strength accompanies desalinization and may elevate the mobility of the landslides.

**Acknowledgements**

This study was partially supported by the National Natural Science Foundation of China (No. 41072213) and the Opening Fund of Key Laboratory of Mechanics on Disaster and Environment in Western China (Lanzhou University) (No. 201207). Support by China Scholarship Council to Fanyu Zhang for his study in Kyoto University is greatly appreciated. The valuable comments by the editor and two referees of this paper are greatly appreciated. Finally, the authors' special thanks go to Mr. William H. Schulz, U.S. Geological Survey, for his great help in revising the manuscript both technically and editorially.

**References**

Anson, R.W.W., Hawkins, A.B., 1998. The effect of calcium ions in pore water on the residual shear strength of kaolinite and sodium montmorillonite. Geotechnique 48, 787-800.

Bishop, A.W., Green, G.E., Garga, V.K., Andresen, A., Brown, J.D., 1971. A new ring shear apparatus and its application to the measurement of residual strength. Geotechnique 21, 273-328.

Bowders, J.J.J., Daniel, D.E., 1987. Hydraulic conductivity of compacted clay to dilute organic chemicals. Journal of geotechnical engineering 117, 1278-1280.

Bromhead, E.N., 1979. A simple ring shear apparatus. Ground Engineering 12, 40-44.

Chen, J., Han, Q., Li, B., 1999. Land surface settlement, soil loss and corresponding harness in Heifangtai Irrigation area in Yongjing County. Soil and Water Conservation in China 4, 15-17.(in Chinese).

Derbyshire, E., 2001. Geological hazards in loess terrain, with particular reference to the loess regions of China. Earth-Science Reviews 54, 231-260.

Derbyshire, E., Dijkstra, T.A., Smalley, I.J., Li, Y., 1994. Failure mechanisms in loess and the effects of moisture content changes on remoulded strength. Quaternary International 24, 5-15.

Di Maio, C., 1996. Exposure of bentonite to salt solution: Osmotic and mechanical effects. Geotechnuque 46, 695-707.

Di Maio, C., 1998. Discussion on exposure of bentonite to salt solution: Osmotic and mechanical effects. Geotechnique 48, 433–436.

Di Maio, C., Fenelli, G.B., 1994. Residual strength of kaolin and bentonite: the influence of their constituent pore fluid. Geotechnique 44, 217-226.

Dieterich, J.H., Kilgore, B.D., 1994. Direct observation of frictional contacts: New insights for state-dependent properties. Pure and Applied Geophysics PAGEOPH 143, 283-302.

Dijkstra, T.A., Rogers, C.D.F., Smalley, I.J., Derbyshire, E., Li, Y.J., Meng, X.M., 1994. The loess of north-central China: Geotechnical properties and their relation to slope stability. Engineering Geology 36, 153-171.

Gajo, A., Maines, M., 2007. Mechanical effects of aqueous solutions of inorganic acids and bases on a natural active clay. Géotechnique 57, 687-699.

Gibbs, H.J., Holland, W.Y., 1960. Petrographic and engineering properties of loess. U.S. Bureau of Reclamation, Denver. Engineering Monographs 28, 1-37.

Gratchev, I.B., Sassa, K., 2009. Cyclic behavior of fine-grained soils at different pH values. Journal of Geotechnical and Geoenvironmental Engineering 135, 271-279.

Ishihara, K., 1993. Liquefaction and flow failure during earthquake. Géotechnique 43, 51-351.

Iverson, N.R., Mann, J.E., Iverson, R.M., 2010. Effects of soil aggregates on debris-flow mobilization: Results from ring-shear experiments. Engineering Geology 114, 84-92.

Kenney, T.C., 1967. The influence of mineralogical composition on the residual strength of natural soils. Proc. Geotech. Conf: on Shear Strength Properties of Natural Soils and Rocks, Oslo, 1, 123-129.

Kestin, J., Khalifa, H.E., Correia, R.J., 1981. Tables of the dynamic and kinematic viscosity of aqueous NaCl solutions in the temperature range 20-150 °C and the pressure range O.1~5 MPa. Journal of Physical and Chemical Reference Data 10, 71-87.

Kramer, S.L., 1988. Triggering of liquefaction flow slides in coastal soil deposits. Engineering Geology 26, 17-31.

Lambe, T., Whitman, R., 1969. Soil Mechanics. John Wiley & Sons, Inc.

Long, J., Li, T., Lei, X., Yang, S., 2007. Study on physical properties of soil in sliding zone of loess landslide. Chinese Journal of Geotechnical Engineering 29, 289-293. (in Chinese).

McDowell, G.R., Bolton, M.D., 1998. On the micromechanics of crushable aggregates. Géotechnique 48, 667-679.

Mitchell, J.K., Soga, K., 2005. Fundamentals of Soil Behavior, 3rd Edition. John Wiley & Sons, Inc.

Moore, R., 1991. The chemical and mineralogical controls upon the residual strength of pure and natural clays. Geotechnique 41, 35–47.

Moore, R., 1992. Discussion on the chemical and mineralogical controls upon the residual strength of pure and natural clays. Geotechnique 42, 151-153.

Mori, R., 1964. Some problems on the chemical stability of soils. Rep., Committee of Soil Chemistry, Association of Electrochemistry, Tokyo.

Oda, M., 1972a. Initial fabrics and their relations to mechanical properties of granular material. Soils and Foundations, 12(1), 17-36.

Oda, M., 1972b. The mechanism of fabric changes during compressional deformation of sand. Soils and Foundations, 12(2), 1-18.

456 Picarelli, L., 2010. Discussion on “A rapid loess flowslide triggered by irrigation in China”
457 by D. Zhang, G. Wang, C. Luo, J. Chen, and Y. Zhou. Landslides.
458 Poulos, S.J., 1981. The steady state of deformation. Journal of the Geotechnical Engineering
459 Division, ASCE 107, 553-562.
460 Poulos, S.J., Castro, G., France, J.W., 1985. Liquefaction evaluation procedure. Journal of
461 geotechnical engineering 111, 772-792.
462 Ramiah, B.K., Dayalu, N.K., Purushothamaraj, P., 1970. Influence of chemicals on the
463 residual strength of silty clays. Soils and foundations 10, 25-36.
464 Santamarina, J.C., Klein, K.A., Wang, Y.H., Prencke, E., 2002. Specific surface:
465 determination and relevance. Canadian Geotechnical Journal 39, 233-241.
466 Sassa, K., 1985. The mechanism of debris flows. In Proceedings of the 11th International
467 Conference on Soil Mechanics and Foundation Engineering, San Francisco, Calif. Vol.
468 3, pp. 1173–1176.
469 Sassa, K., Fukuoka, H., Wang, G., Ishikawa, N., 2004. Undrained dynamic-loading
470 ring-shear apparatus and its application to landslide dynamics. Landslides 1, 7-19.
471 Sassa, K., Wang, G., Fukuoka, H., 2003. Performing undrained shear tests on saturated
472 sands in a new intelligent type of ring shear apparatus. Geotechnical Testing Journal 26,
473 257-265.
474 Sridharan, A., Jayadeva, M. S., 1982. Double layer theory and compressibility of clays.
475 Geotechnique 32(2), 133-144.
476 Sridharan, A., Prakash, K., 1999. Influence of clay mineralogy and pore-medium chemistry
477 on clay sediment formation. Canadian Geotechnical Journal 36(5), 961-966.
478 Steward, H.E., Cripps, J.C., 1983. Some engineering implications of chemical weathering of
479 pyritic shale. Quarterly Journal of Engineering Geology and Hydrogeology 16,
480 281-289.
481 Tatsuoka, F., Ochi, K., Fujii, S., Okamoto, M., 1986. Cyclic undrained triaxial and torsional
482 shear strength of sands for different sample preparation methods. Soils and Foundations,
483 6(3): 23-41

484 Tiwari, B., Tuladhar, G.R., Marui, H., 2005. Variation in residual shear strength of the soil
485 with the salinity of pore fluid. Journal of Geotechnical and Geoenvironmental
486 Engineering 131, 1445-1456.
487 Wahid, A.S., Gajo, A., Di Maggio, R., 2011. Chemo-mechanical effects in kaolinite. Part 1:
488 Prepared samples. Geotechnique 61, 439-447.
489 Wang, G., Sassa, K., 2002. Post-failure mobility of saturated sands in undrained
490 load-controlled ring shear tests. Canadian Geotechnical Journal 39, 821-837.
491 Wang, G., Sassa, K., 2009. Seismic loading impacts on excess pore-water pressure maintain
492 landslide triggered flowslides. Earth Surface Processes and Landforms 34, 232-241.
493 Wang, G., Sassa, K., Fukuoka, H., Tada, T., 2007. Experimental study on the shearing
494 behavior of saturated silty soils based on ring-shear tests. Journal of Geotechnical and
495 Geoenvironmental Engineering 133, 319-333.
496 Wang, G., Suemine, A., Schulz, W.H., 2010. Shear-rate-dependent strength control on the
497 dynamics of rainfall-triggered landslides, Tokushima Prefecture, Japan. Earth Surface
498 Processes and Landforms 35, 407-416.
499 Wang, Z., Wu, W., Zhou, Z., 2004. Landslide induced by over-irrigation in loess platform
500 areas in Gansu Province. The Chinese Journal of Geological Hazard and Control 15,
501 43-46. (in Chinese).
502 Wen, B.P., He, L., 2012. Influence of Lixiviation by Irrigation Water on Residual Shear
503 Strength of Weathered Red Mudstone in Northwest China: Implication for its role in
504 landslides' reactivation. Engineering Geology, doi: 10.1016/j.enggeo.2012.08.005 (in
505 press)
506 Xu, L., Dai, F., Gong, Q., Tham, L., Min, H., 2011a. Irrigation-induced loess flow failure in
507 Heifangtai Platform, North-West China. Environmental Earth Sciences, 1-7.
508 Xu, L., Dai, F.C., Tham, L.G., Tu, X.B., Min, H., Zhou, Y.F., Wu, C.X., Xu, K., 2011b.
509 Field testing of irrigation effects on the stability of a cliff edge in loess, North-west
510 China. Engineering Geology 120, 10-17.

511 Yamamuro J.A., Lade P.V., 1999. Experiments and modelling of silty sands susceptible to
512 static liquefaction. Mechanics of Cohesive-Frictional Materials 4: 545-564.
513 Zhang, D., Wang, G., 2007. Study of the 1920 Haiyuan earthquake-induced landslides in
514 loess (China). Engineering Geology 94, 76-88.
515 Zhang, D., Wang, G., Luo, C., Chen, J., Zhou, Y., 2009. A rapid loess flowslide triggered
516 by irrigation in China. Landslides 6, 55-60.
517 Zhang, H., Han, S., 1996. Viscosity and density of water + sodium chloride + potassium
518 chloride solutions at 298.15 K. Journal of Chemical & Engineering Data 41, 516-520.
519 Zhang, Y., 2007. Systematic analysis on loess landslides in Heifangtai, Gansu Province,
520 China. Thesis submitted to Northwest University for Master's degree. (in Chinese).
521 Zlatovic, S., Ishihara, K., 1997. Normalized behavior of very loose non-plastic soils: effects of
522 fabric. Soils and Foundations, 37(4):47-56.

## **Captions**:

Fig. 1. (a) Location of study site; (b) a wide view of the landslides in Heifangtai area; (c) close-up view of a landslide that reactivated in 2008 (Photos on July 15, 2008).

Fig. 2. Lithological profile of Heifangtai area

Fig. 3. (a) Wide view of Heifangtai side slope area during winter with salt deposition (white colored parts); (b) Close-up view of the salt deposition (Photos on November 12, 2011).

Fig. 4. Grain size distribution of loess sample

Fig. 5. Ring-shear apparatus DPRI-Ver.5. (a) Overview; (b) sample in ring-shear box; (c) cross section through the center of the shear box

Fig. 6. Undrained ring shear test on sample saturated by distilled de-aired water ($T_1$). (a) Normal stress, pore pressure, and shear resistance against shear displacement; (b) time series data; (c) effective stress path. F indicates conditions at failure and SSP indicates steady-state conditions.

Fig. 7. Undrained ring shear test on sample saturated by de-aired solution with NaCl concentration being 12% ($T_5$). (a) Normal stress, pore pressure, and shear resistance against shear displacement; (b) time series data; (c) effective stress path. F indicates conditions at failure and SSP indicates steady-state conditions.

Fig. 8. Undrained ring shear test ($T_{11}$) on the desalinized sample that was retrieved from test $T_5$. (a) Normal stress, pore pressure, and shear resistance against shear displacement; (b) time series data; (c) effective stress path. F indicates conditions at failure and SSP indicates steady-state conditions.

Fig. 9. Undrained shear test results for samples saturated by de-aired solution with different NaCl concentrations ($T_1$-$T_7$). (a) Shear resistance versus shear displacement; (b) monitored pore-water pressure versus shear displacement; (c) effective stress paths.

Fig. 10. Undrained shear test results for desalinized retrieved samples ($T_8$-$T_{13}$) and the original sample ($T_1$). (a) Shear resistance versus shear displacement; (b) pore pressure versus shear displacement; (c) effective stress paths. NaCl concentrations prior to desalinization and testing are indicated.

Fig. 11. Undrained peak shear strength and shear strength at steady state against NaCl concentrations (tests $T_1$-$T_7$ in Table 3).

Fig. 12. Results of undrained shear tests on the desalinized samples that were retrieved from tests T2-T7. Here the initial NaCl concentration (%) indicates that of the solution used to saturate the samples in T2-T7, respectively.

Fig. 13. SEM imaging of the samples saturated by different NaCl concentrations: (a) 0%; (b) 10%; (c) 12%; (d) 16%

Fig. 14. Liquid limit against NaCl concentration

Table 1. Chemical composition of irrigation water, spring water, groundwater and loess in Heifangtai area

| Ion type | Irrigation water (Chen et al., 1999) | | Spring water (Chen et al., 1999) | | Groundwater (Chen et al., 1999) | | Loess | |
|---|---|---|---|---|---|---|---|---|
| | mg/l | % | mg/l | % | mg/l | % | mg/kg | % |
| $Na^{+}$ | 8.74 | 3.12 | 17112.24 | 30.02 | 13176.4 | 28.63 | 2521 | 31.09 |
| $K^{+}$ | 2.6 | 0.93 | 28.03 | 0.05 | 23.8 | 0.05 | 20 | 0.25 |
| $Ca^{2+}$ | 45.53 | 16.26 | 1077.48 | 1.89 | 873.74 | 1.90 | 204 | 2.52 |
| $Mg^{2+}$ | 16.58 | 5.92 | 2614.41 | 4.59 | 1999.09 | 4.34 | 93 | 1.15 |
| $Cl^{-}$ | 43.68 | 15.60 | 27677.56 | 48.55 | 21464.98 | 46.64 | 2629 | 32.42 |
| $SO_4^{2-}$ | 34.39 | 12.28 | 8424.46 | 14.78 | 8386.04 | 18.22 | 2450 | 30.22 |
| $HCO^{3-}$ | 128.53 | 45.90 | 75.1 | 0.13 | 98.96 | 0.22 | 191 | 2.36 |
| Sum | 280.5 | 100.00 | 57009.08 | 100.00 | 46023.01 | 100.00 | 8108.00 | 100.00 |
| PH | 8.46 | | 7.94 | | 7.90 | | 8.16 | |

Table 2. Some physical properties of loess used in this study

| Property | Value |
|---|---|
| Specific gravity (Gs) | 2.76 |
| Initial moist bulk density (g/cm3) | 1.53 |
| Initial water content (%) | 6.50 |
| Initial void ratio | 1.05 |
| Liquid limit (%) | 26.55 |
| Plastic limit (%) | 15.98 |
| Plasticity index (%) | 10.57 |

Table 3. Summary of ring-shear test results

| Test No. | Consolidated state | | | | | | State value | |
|---|---|---|---|---|---|---|---|---|
| | s | $\rho_d$ | e | $B_D$ | $\sigma_i$ | $\tau_i$ | $\tau_p$ | $\tau_r$ |
| Saturated by solutions with differing NaCl by weight | | | | | | | | |
| $T_1$ | 0 | 1.577 | 0.750 | 0.98 | 250 | 0 | 71.9 | 32.0 |
| $T_2$ | 3 | 1.577 | 0.750 | 1.00 | 250 | 0 | 74.6 | 40.4 |
| $T_3$ | 6 | 1.573 | 0.754 | 1.00 | 250 | 0 | 79.6 | 47.6 |
| $T_4$ | 10 | 1.575 | 0.753 | 1.00 | 250 | 0 | 78.7 | 48.6 |
| $T_5$ | 12 | 1.575 | 0.753 | 1.00 | 250 | 0 | 125.9 | 57.7 |
| $T_6$ | 14 | 1.577 | 0.750 | 0.98 | 250 | 0 | 91.5 | 52.9 |
| $T_7$ | 16 | 1.575 | 0.752 | 0.99 | 250 | 0 | 68.3 | 23.4 |
| $T_7$’ | 16 | 1.593 | 0.733 | 0.99 | 250 | 0 | 82.6 | 33.6 |
| Desalinization | | | | | | | | |
| $T_8$ | 3* | 1.576 | 0.751 | 1.00 | 250 | 0 | 72.5 | 31.5 |
| $T_9$ | 6* | 1.579 | 0.748 | 0.98 | 250 | 0 | 68.7 | 34.2 |
| $T_{10}$ | 10* | 1.578 | 0.749 | 1.00 | 250 | 0 | 66.1 | 29.9 |
| $T_{11}$ | 12* | 1.580 | 0.747 | 1.00 | 250 | 0 | 72.0 | 31.5 |
| $T_{12}$ | 14* | 1.578 | 0.749 | 1.00 | 250 | 0 | 71.4 | 32.0 |
| $T_{13}$ | 16* | 1.577 | 0.750 | 1.00 | 250 | 0 | 68.8 | 31.5 |

Note: All stress in kPa. s: NaCl concentration (3 denotes 3% of NaCl in the solution by weight; 3* denotes that the sample was retrieved from the former test that used a solution with 3% of NaCl by weight); $\rho_d$: dry density; e: void ratio after consolidation; $B_D$: parameter of saturation; $\sigma_i$: initial normal stress; $\tau_i$: initial shear stress; $\tau_p$: peak shear strength; $\tau_r$: shear strength at steady-state.

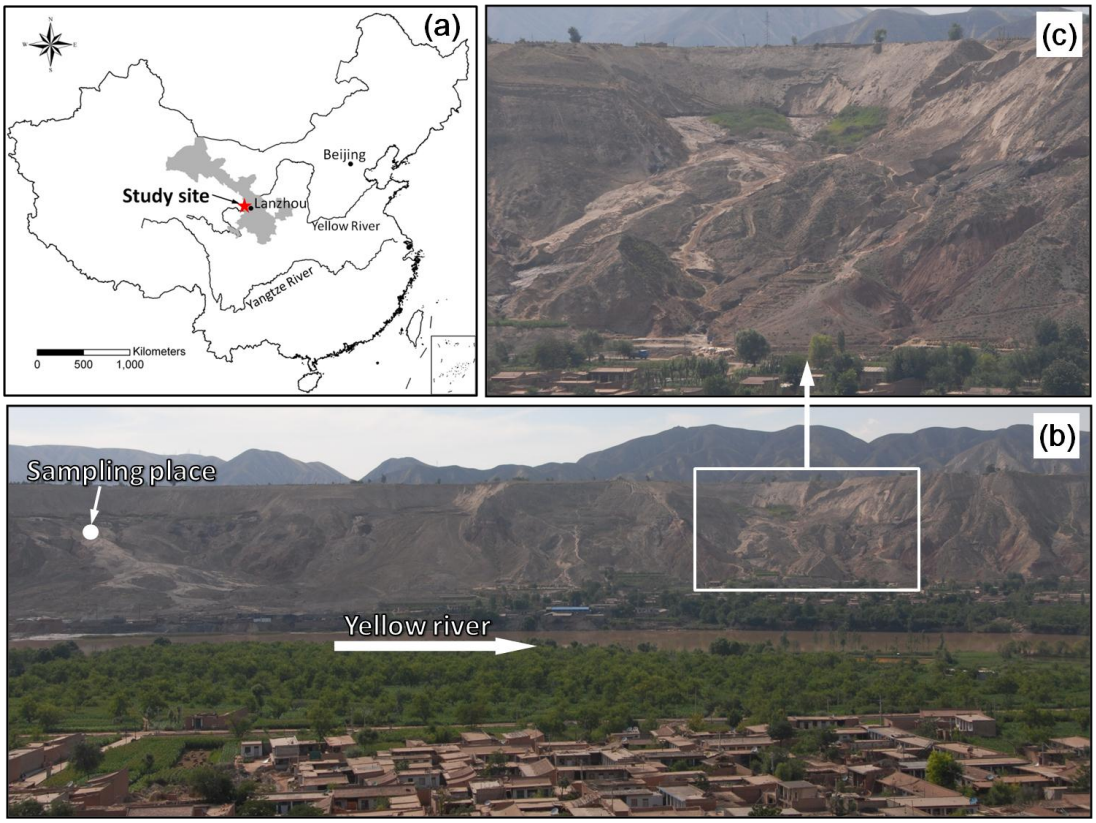


Fig. 1. (a) Location of study site; (b) a wide view of the landslides in Heifangtai area; (c) close-up view of a landslide that reactivated in 2008 (Photos on July 15, 2008).

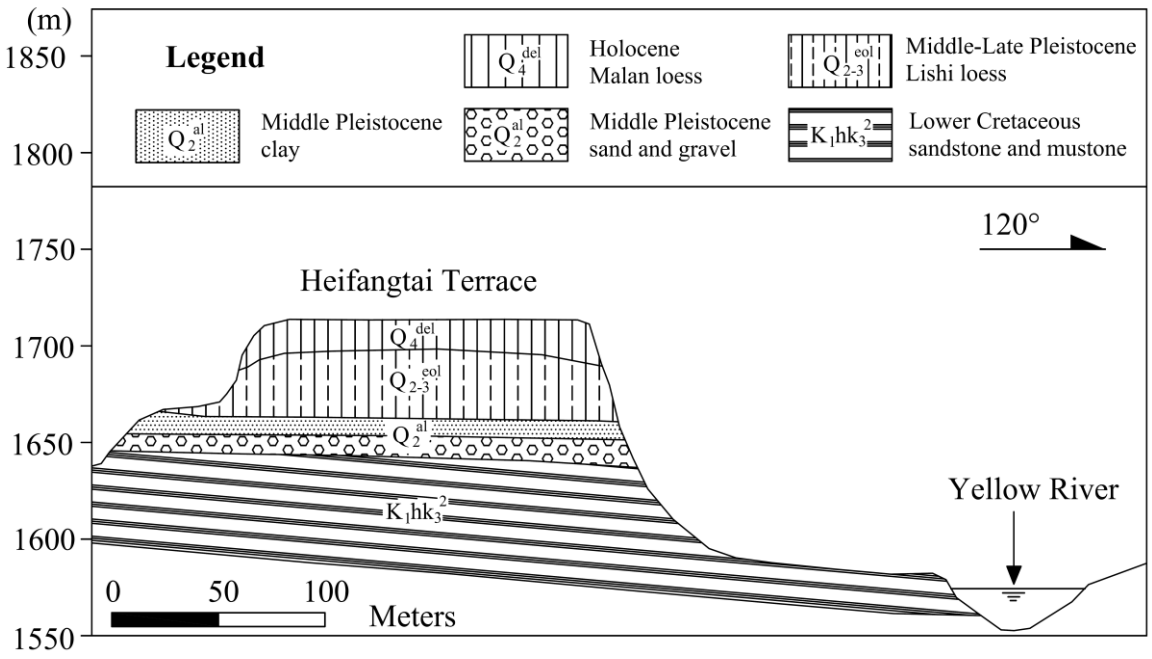


Fig. 2. Lithological profile of Heifangtai area

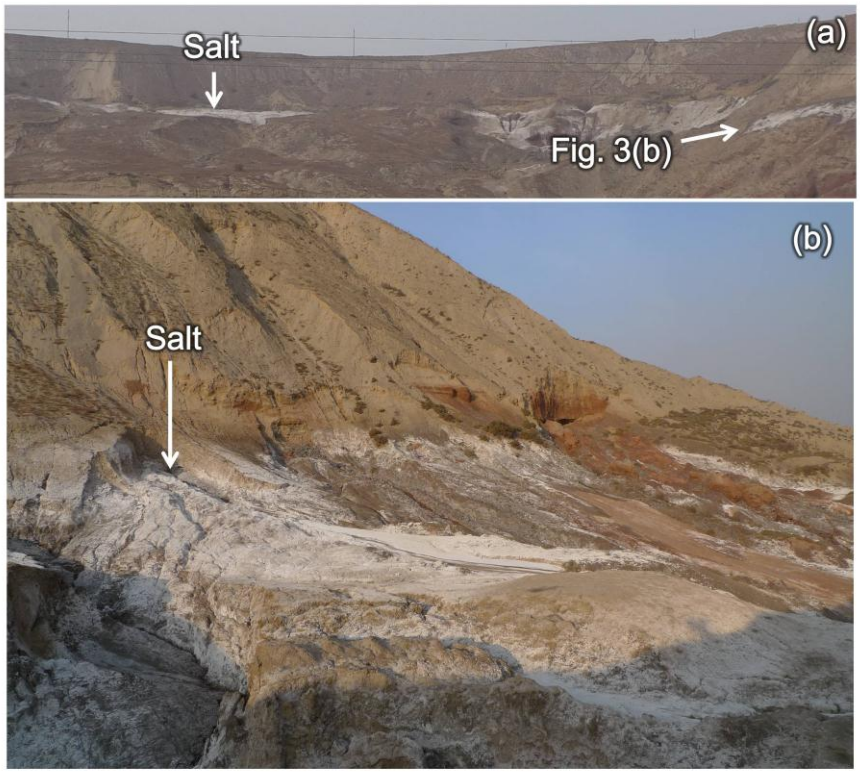


Fig. 3. (a) Wide view of Heifangtai side slope area on winter with salt deposition (white colored parts); (b) Close-up view of the salt deposition (Photos on November 12, 2011).

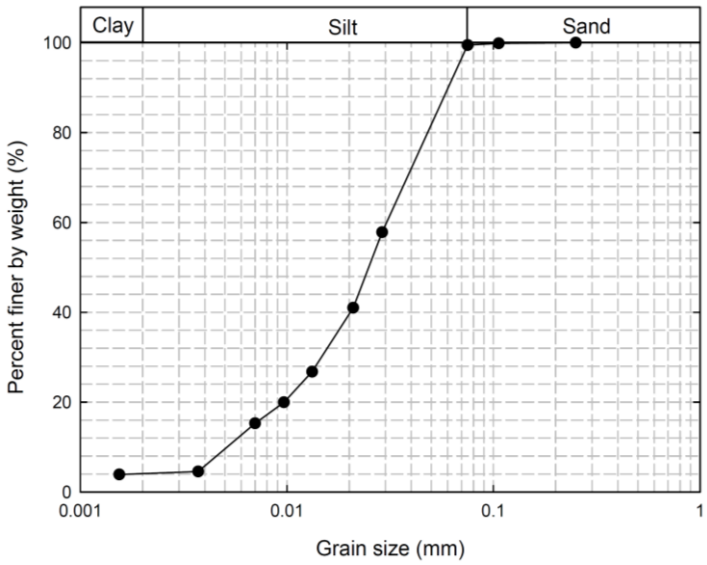


Fig. 4. Grain size distribution of loess sample

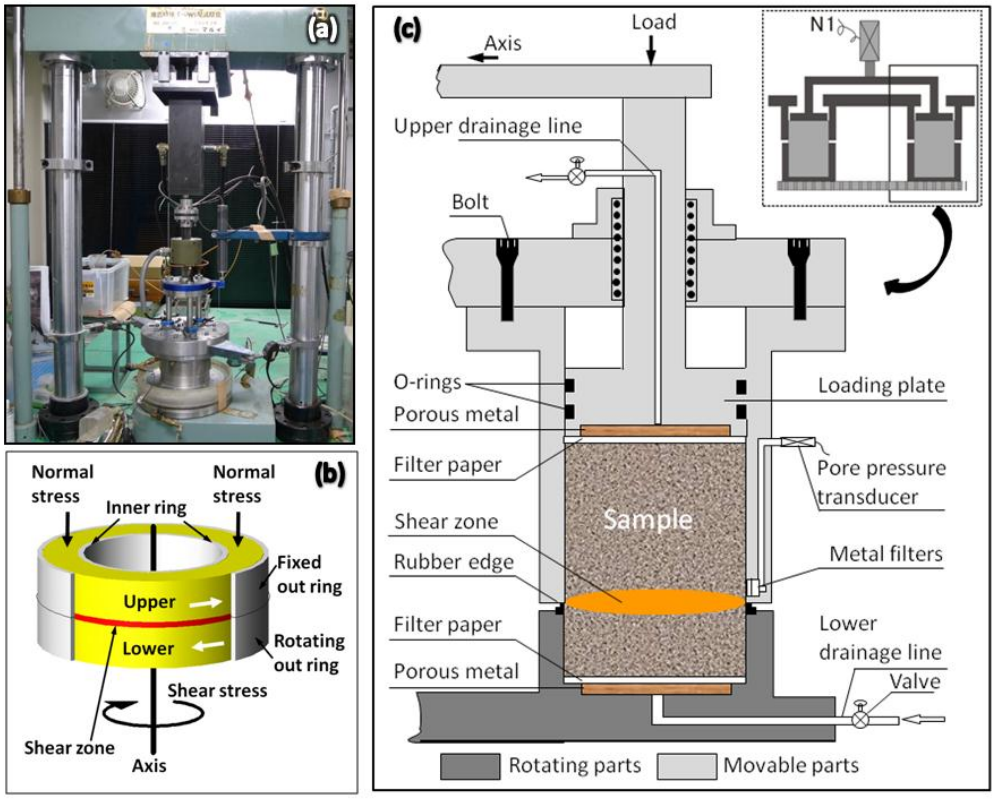


Fig. 5. Ring-shear apparatus DPRI-Ver.5. (a) Overview; (b) sample in ring-shear box; (c) half of the cross section through center of undrained shear box

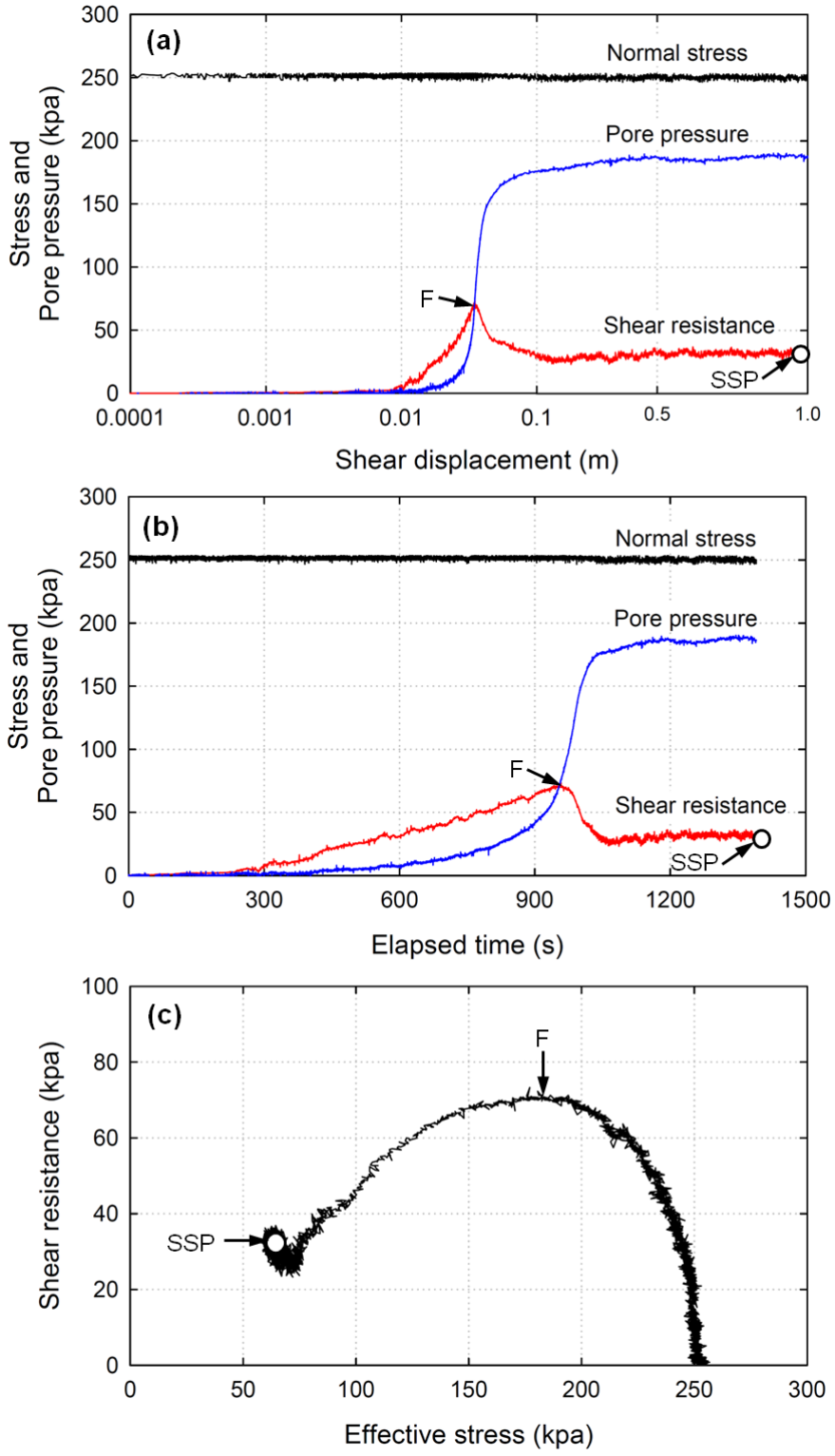


Fig. 6. Undrained ring shear test on sample saturated by distilled de-aired water ($T_1$). (a) Normal stress, pore pressure, and shear resistance against shear displacement; (b) time series data; (c) effective stress path.

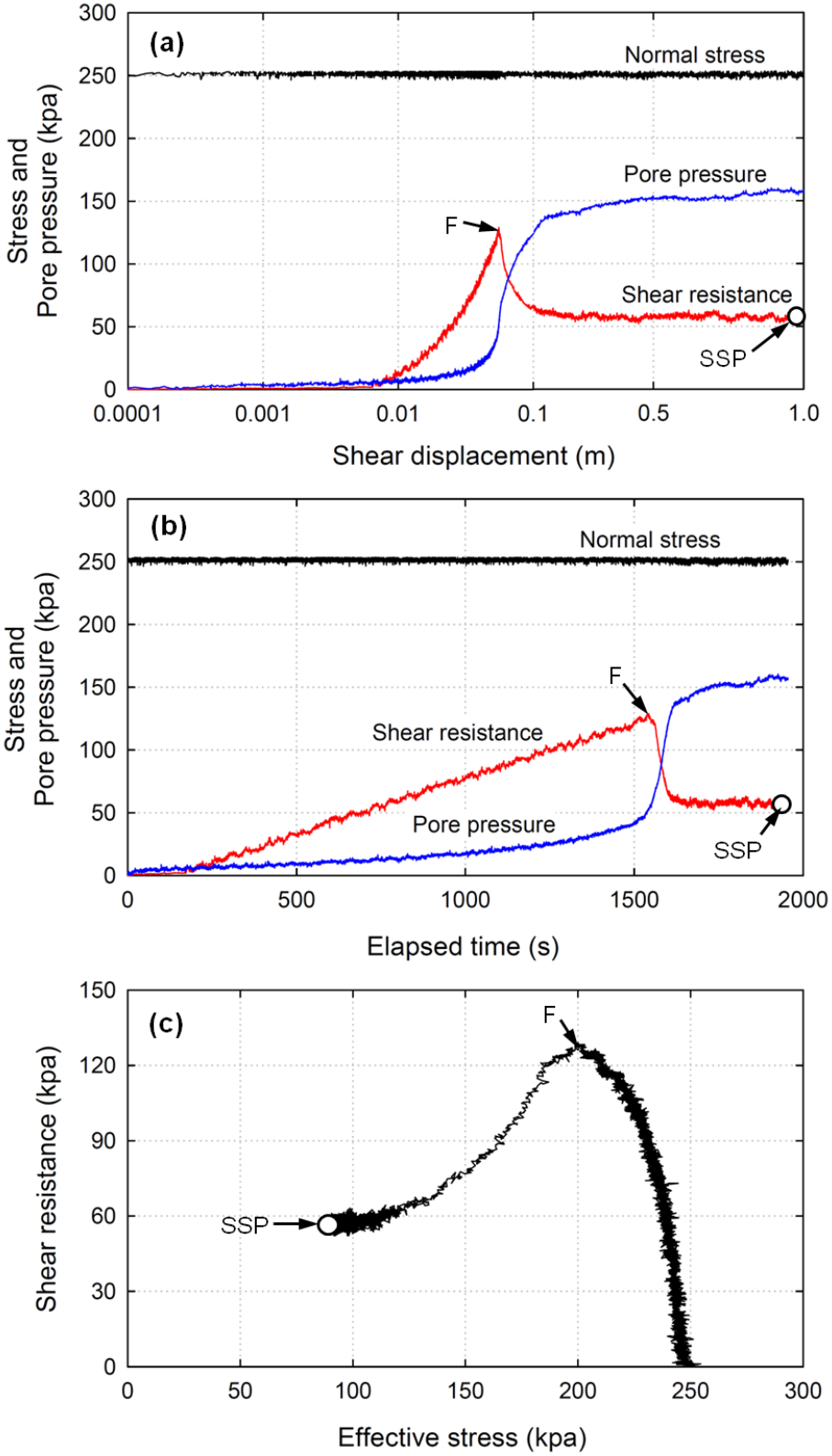


Fig. 7. Undrained ring shear test on sample saturated by de-aired solution with NaCl concentration being 12% ($T_5$). (a) Normal stress, pore pressure, and shear resistance against shear displacement; (b) time series data; (c) effective stress path.

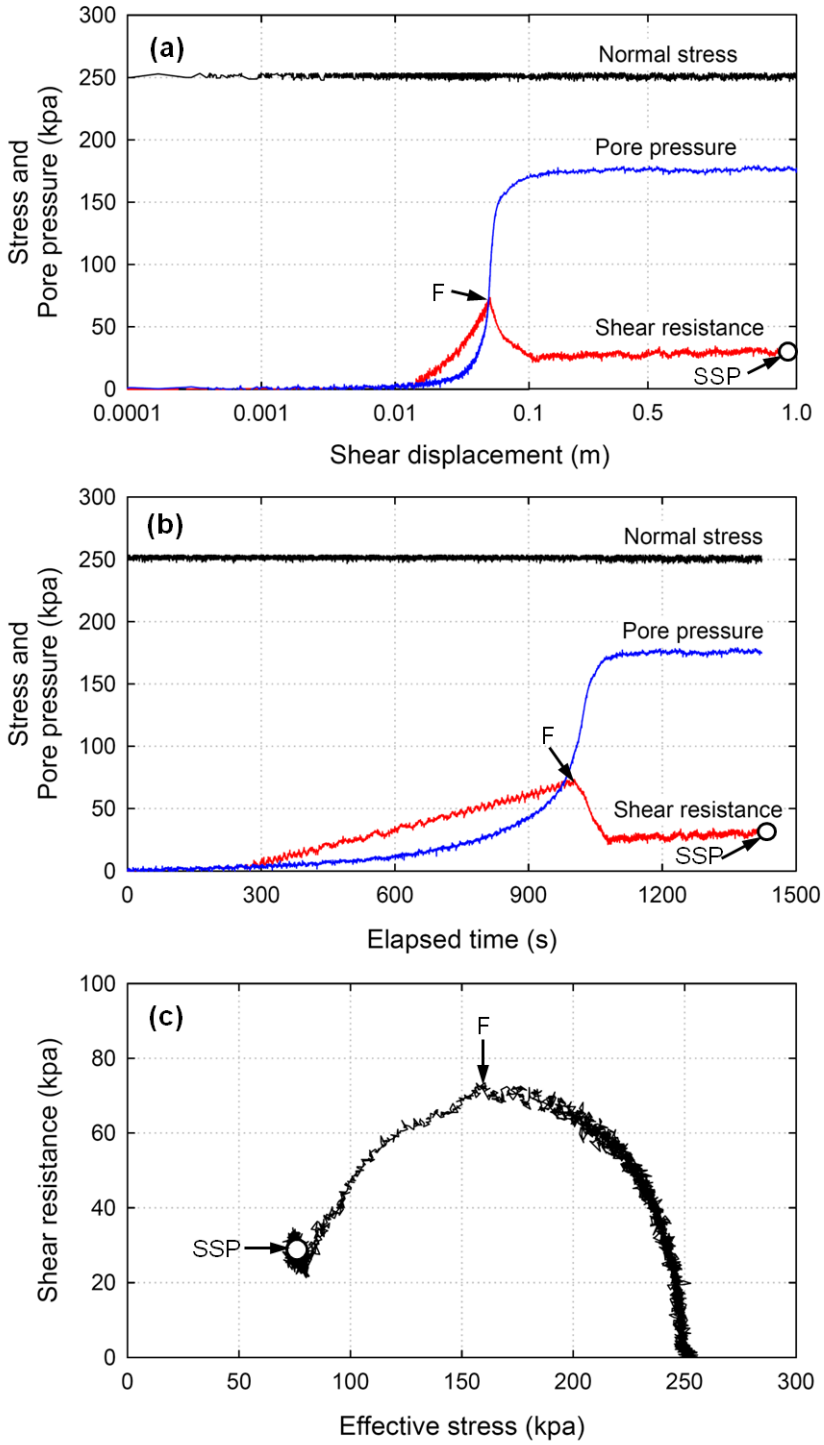


Fig. 8. Undrained ring shear test ($T_{11}$) on the desalinized sample that was retrieved from test $T_5$. (a) Normal stress, pore pressure, and shear resistance against shear displacement; (b) time series data; (c) effective stress path.

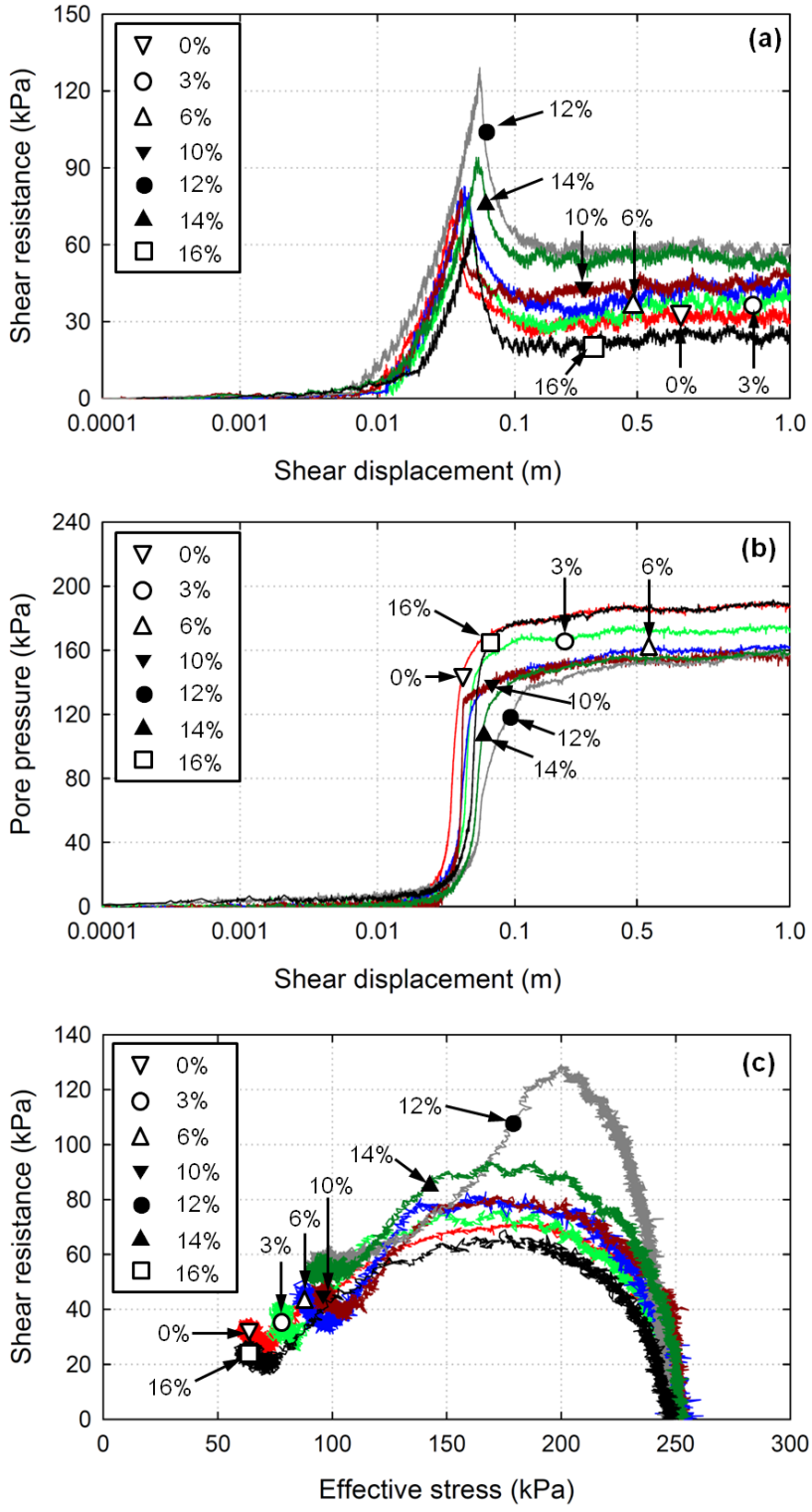


Fig. 9. Undrained shear test results for samples saturated by de-aired solution with different NaCl concentrations ($T_1$-$T_7$). (a) Shear resistance versus shear displacement; (b) monitored pore-water pressure versus shear displacement; (c) effective stress paths.

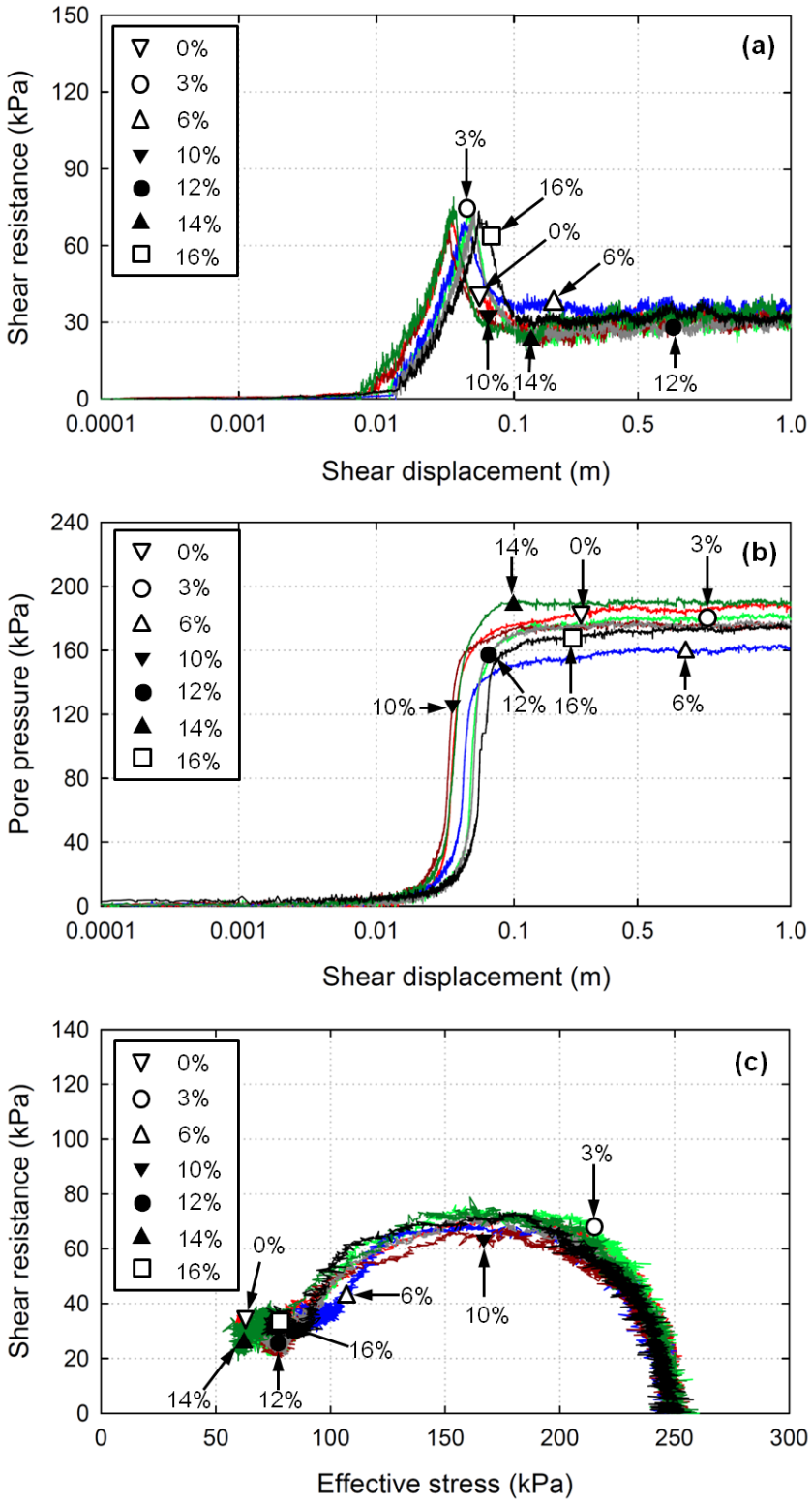


Fig. 10. Undrained shear test results for retrieved samples ($T_8$-$T_{13}$) and the original sample ($T_1$). (a) Shear resistance versus shear displacement; (b) pore pressure versus shear displacement; (c) effective stress path

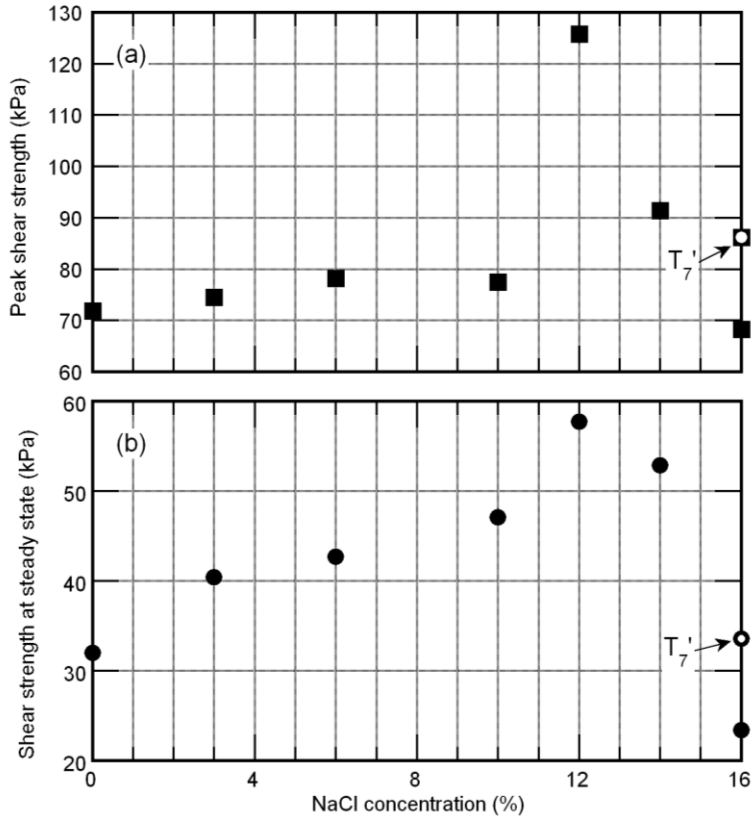


Fig. 11. Undrained peak shear strength (a), and shear strength at steady state (b), against NaCl concentrations (tests $T_1$-$T_7$ in Table 3).

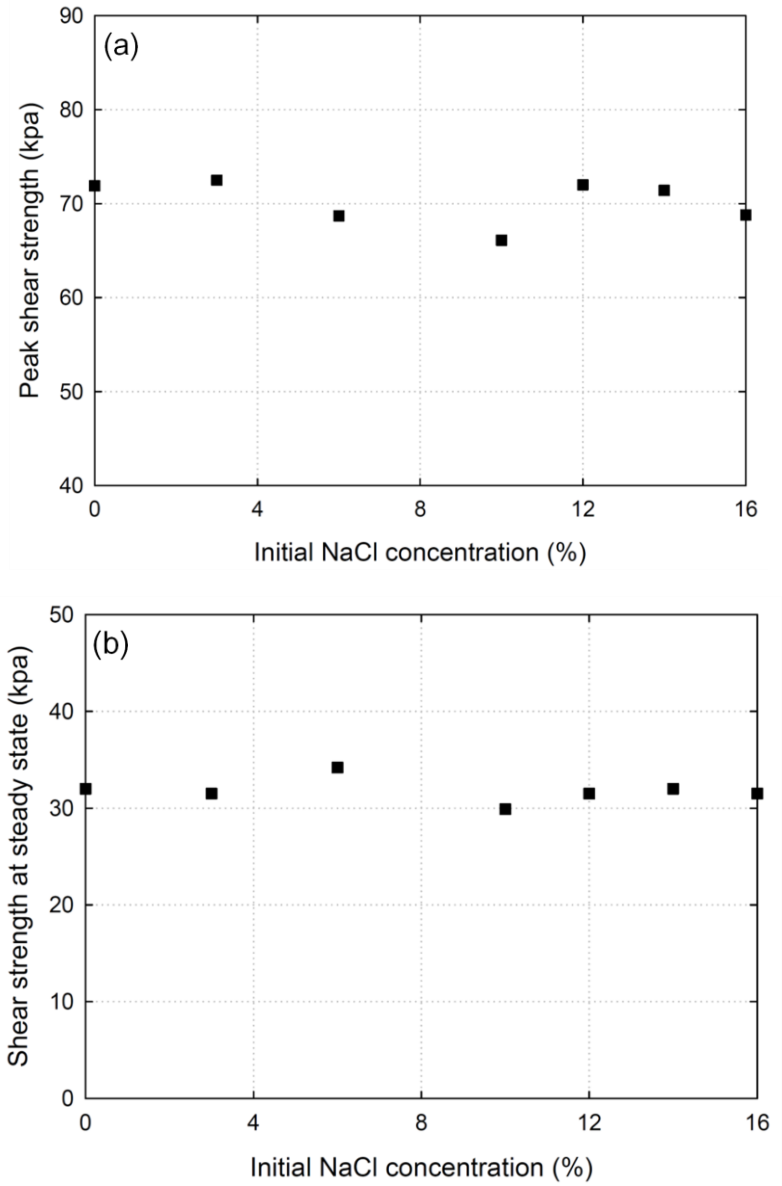


Fig. 12. Results of undrained shear tests on the desalinized samples that were retrieved from tests T2~T7. Here the initial NaCl concentration (%) indicts that of the solution used to saturate the samples in T2~T7, respectively. (a) Peak shear strength; (b) shear strength at steady state.

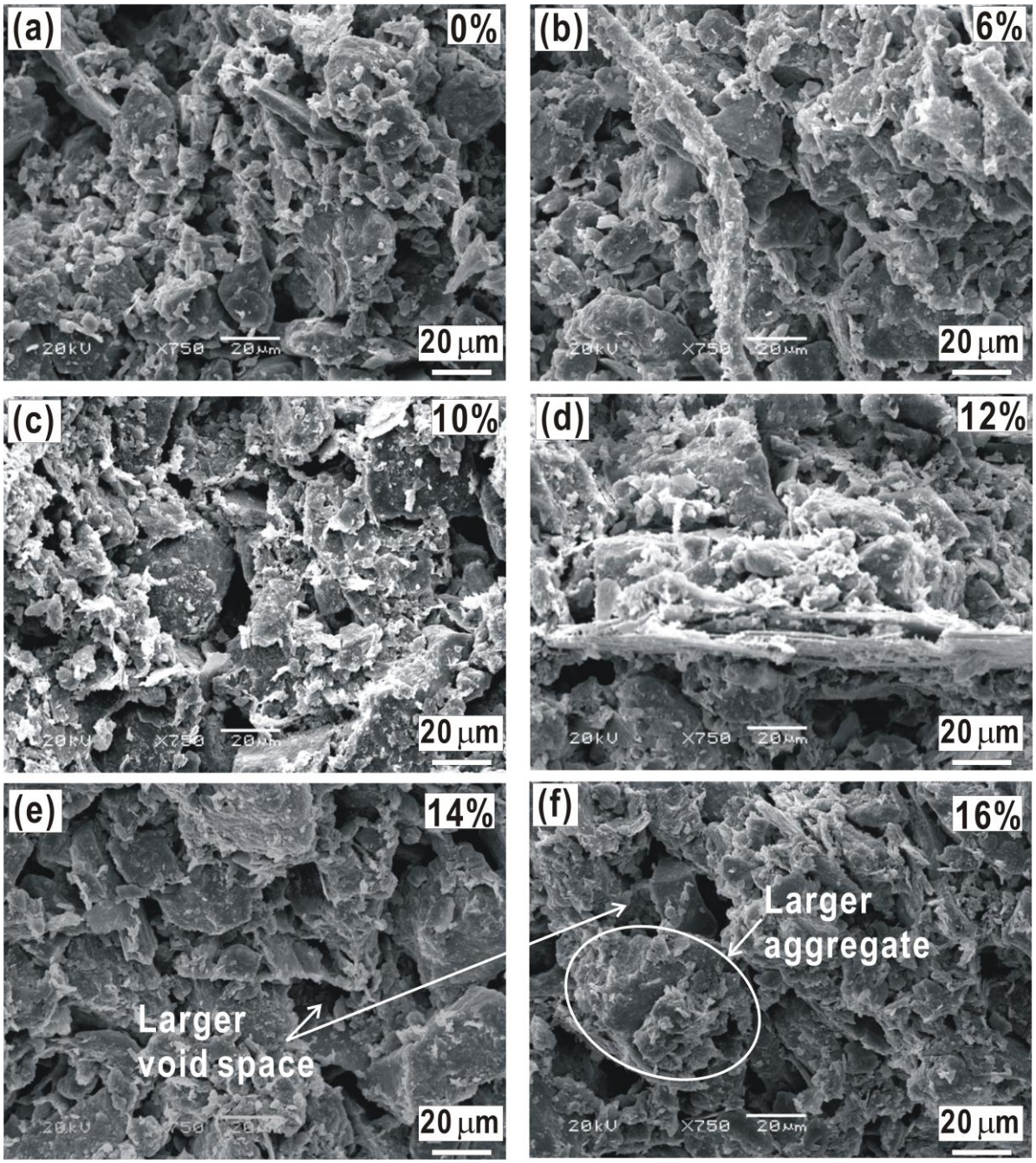


Fig. 13. SEM images of the samples saturated by different NaCl concentrations. (a) 0%; (b) 6%, (c) 10%; (d) 12%; (e) 12%, and (f) 16%.

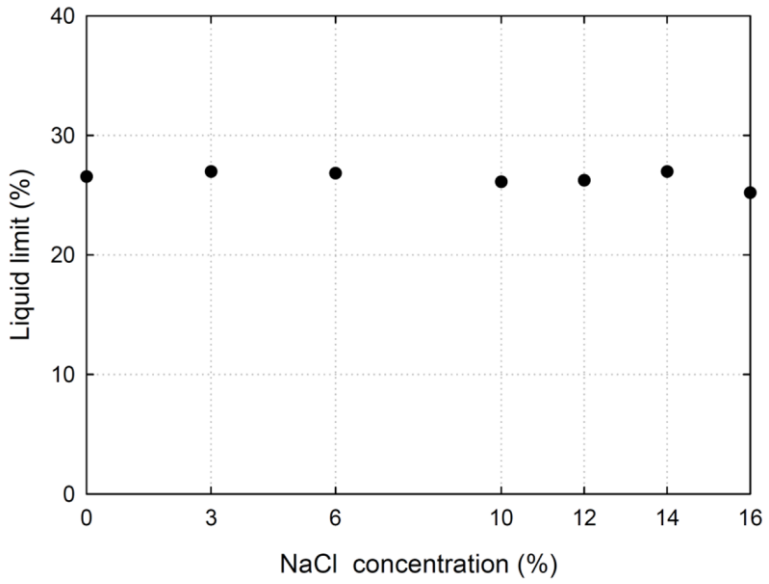


Fig. 14. Liquid limit against NaCl concentration